JOURNAL OF
Applied Polymer
SCIENCE

Special Issue: Polymers for Microelectronics

Guest Editors: Dr Brian Knapp (Promerus LLC) and
Prof. Paul A. Kohl (Georgia Institute of Technology)

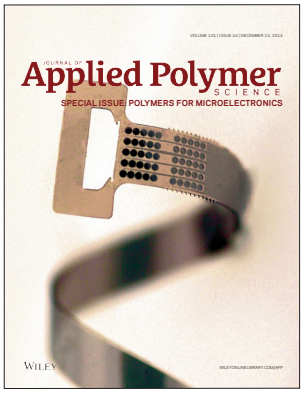

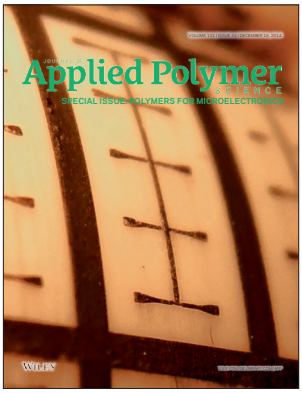

EDITORIAL

Polymers for Microelectronics
B. Knapp and P. A. Kohl, *J. Appl. Polym. Sci.* 2014, **DOI: 10.1002/app.41233**

REVIEW

Negative differential conductance materials for flexible electronics
A. Nogaret, *J. Appl. Polym. Sci.* 2014, **DOI: 10.1002/app.40169**

RESEARCH ARTICLES

Generic roll-to-roll compatible method for insolubilizing and stabilizing conjugated active layers based on low energy electron irradiation
M. Helgesen, J. E. Carlé, J. Helt-Hansen, A. Miller, and F. C. Krebs, *J. Appl. Polym. Sci.* 2014, **DOI: 10.1002/app.40795**

Selective etching of polylactic acid in poly(styrene)-block-poly(D,L)lactide diblock copolymer for nanoscale patterning
C. Cummins, P. Mokarian-Tabari, J. D. Holmes, and M. A. Morris, *J. Appl. Polym. Sci.* 2014, **DOI: 10.1002/app.40798**

Preparation and dielectric behavior of polyvinylidene fluoride composite filled with modified graphite nanoplatelet
P. Xie, Y. Li, and J. Qiu, *J. Appl. Polym. Sci.* 2014, **DOI: 10.1002/app.40229**

Design of a nanostructured electromagnetic polyaniline–Keggin iron–clay composite modified electrochemical sensor for the nanomolar detection of ascorbic acid
R. V. Lilly, S. J. Devaki, R. K. Narayanan, and N. K. Sadanandhan, *J. Appl. Polym. Sci.* 2014, **DOI: 10.1002/app.40936**

Synthesis and characterization of novel phosphorous-silicone-nitrogen flame retardant and evaluation of its flame retardancy for epoxy thermosets
Z.-S. Li, J.-G. Liu, T. Song, D.-X. Shen, and S.-Y. Yang, *J. Appl. Polym. Sci.* 2014, **DOI: 10.1002/app.40412**

Electrical percolation behavior and electromagnetic shielding effectiveness of polyimide nanocomposites filled with carbon nanofibers
L. Nayak, T. K. Chaki, and D. Khastgir, *J. Appl. Polym. Sci.* 2014, **DOI: 10.1002/app.40914**

Morphological influence of carbon modifiers on the electromagnetic shielding of their linear low density polyethylene composites
B. S. Villacorta and A. A. Ogale, *J. Appl. Polym. Sci.* 2014, **DOI: 10.1002/app.41055**

Electrical and EMI shielding characterization of multiwalled carbon nanotube/polystyrene composites
V. K. Sachdev, S. Bhattacharya, K. Patel, S. K. Sharma, N. C. Mehra, and R. P. Tandon, *J. Appl. Polym. Sci.* 2014, **DOI: 10.1002/app.40201**

Anomalous water absorption by microelectronic encapsulants due to hygrothermal-induced degradation
M. van Soestbergen and A. Mavinkurve, *J. Appl. Polym. Sci.* 2014, **DOI: 10.1002/app.41192**

Design of cyanate ester/azomethine/ZrO_2 nanocomposites high-k dielectric materials by single step sol-gel approach
M. Ariraman, R. Sasi Kumar and M. Alagar, *J. Appl. Polym. Sci.* 2014, **DOI: 10.1002/app.41097**

Furan/imide Diels–Alder polymers as dielectric materials
R. G. Lorenzini and G. A. Sotzing, *J. Appl. Polym. Sci.* 2014, **DOI: 10.1002/app.40179**

High dielectric constant polyimide derived from 5,5'-bis[(4-amino) phenoxy]-2,2'-bipyrimidine
X. Peng, Q. Wu, S. Jiang, M. Hanif, S. Chen, and H. Hou, *J. Appl. Polym. Sci.* 2014, **DOI: 10.1002/app.40828**

The influence of rigid and flexible monomers on the physical-chemical properties of polyimides
T. F. da Conceição and M. I. Felisberti, *J. Appl. Polym. Sci.* 2014, **DOI: 10.1002/app.40351**

JOURNAL OF
Applied Polymer
SCIENCE

Special Issue: Polymers for Microelectronics

Guest Editors: Dr Brian Knapp (Promerus LLC) and
Prof. Paul A. Kohl (Georgia Institute of Technology)

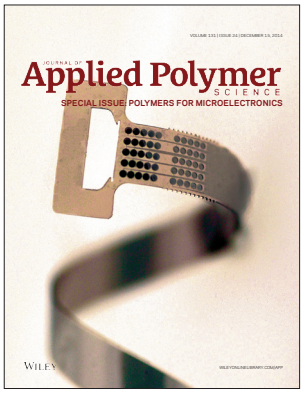

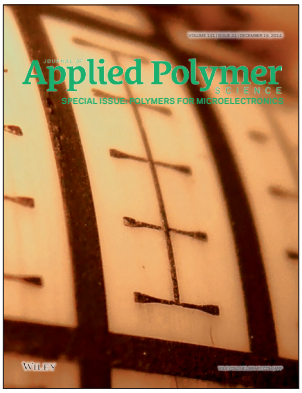

Development of polynorbornene as a structural material for microfluidics and flexible BioMEMS
A. E. Hess-Dunning, R. L. Smith, and C. A. Zorman, *J. Appl. Polym. Sci.* 2014, **DOI:** 10.1002/app.40969

A thin film encapsulation layer fabricated via initiated chemical vapor deposition and atomic layer deposition
B. J. Kim, D. H. Kim, S. Y. Kang, S. D. Ahn, and S. G. Im, *J. Appl. Polym. Sci.* 2014, **DOI:** 10.1002/app.40974

Surface relief gratings induced by pulsed laser irradiation in low glass-transition temperature azopolysiloxanes
V. Damian, E. Resmerita, I. Stoica, C. Ibanescu, L. Sacarescu, L. Rocha, and N. Hurduc, *J. Appl. Polym. Sci.* 2014, **DOI:** 10.1002/app.41015

Polymer-based route to ferroelectric lead strontium titanate thin films
M. Benkler, J. Hobmaier, U. Gleißner, A. Medesi, D. Hertkorn, and T. Hanemann, *J. Appl. Polym. Sci.* 2014, **DOI:** 10.1002/app.40901

The influence of dispersants that contain polyethylene oxide groups on the electrical resistivity of silver paste
T. H. Chiang, Y.-F. Chen, Y. C. Lin, and E. Y. Chen, *J. Appl. Polym. Sci.* 2014, **DOI:** 10.1002/app.41183

Quantitative investigation of the adhesion strength between an SU-8 photoresist and a metal substrate by scratch tests
X. Zhang, L. Du, and M. Zhao, *J. Appl. Polym. Sci.* 2014, **DOI:** 10.1002/app.41108

Thermodynamic and kinetic aspects of defectivity in directed self-assembly of cylinder-forming diblock copolymers in laterally confining thin channels
B. Kim, N. Laachi, K. T. Delaney, M. Carilli, E. J. Kramer, and G. H. Fredrickson, *J. Appl. Polym. Sci.* 2014, **DOI:** 10.1002/app.40790

JOURNAL OF Applied Polymer SCIENCE

Electrical and EMI Shielding Characterization of Multiwalled Carbon Nanotube/Polystyrene Composites

Virendra Kumar Sachdev,[1] Sudeshna Bhattacharya,[1] Kamlesh Patel,[2] Surender Kumar Sharma,[1] Navin Chand Mehra,[1] Ram Pal Tandon[1]

[1]Department of Physics and Astrophysics, University of Delhi, Delhi, India

[2]Department of Electronic Science, University of Delhi South Campus, New Delhi, India

Correspondence to: V. K. Sachdev (E-mail: vk_sachdev@yahoo.com)

ABSTRACT: The electromagnetic interference (EMI) shielding mechanism of carbon nanotube (CNT)/polymer nanocomposites synthesized through a unique processing technique has been studied. As CNT/polymer nanocomposites evolve towards device applications, homogenous dispersion of CNTs has become a main objective to realize their full potential. In this work, dispersion of multi-walled carbon nanotubes (MWCNTs) in polystyrene (PS) powder via dry state tumble mixing has been carried out. This involves the coating of the PS particles with the MWCNTs. Pellets were prepared by hot compression of resulted mixture. Conductivity behavior has shown that an extremely small mass fraction of 0.05 wt % MWCNTs in PS is good enough for percolation threshold. A detailed study of EMI shielding behavior of these composites is reported in addition to physical phenomena involved. The shielding effectiveness achieved is higher compared to solution mixing technique used by others. Decrease in hardness with increase in MWCNT content is little. Scanning electron microscope studies of these nanocomposites revealed a web/mesh like structure consisting of MWCNTs.
 J. Appl. Polym. Sci. **2014**, *131*, 40201.

KEYWORDS: composites; graphene and fullerenes; mechanical properties; nanotubes; polystyrene

Received 14 September 2013; accepted 14 November 2013

DOI: 10.1002/app.40201

INTRODUCTION

Polymer composites filled with nanosized fillers have generated a significant scientific interest in the recent years due to their unique electrical, thermal, and mechanical properties.[1–4] The nanosized fillers in such composites provide huge interfacial area. Additionally, the high aspect ratio (length to diameter ratio) of nanomaterials allows property enhancement at lower concentrations compared to conventional fillers.[5–7] Such composites offer variety of applications in high strength materials, biomedical engineering appliances, electrostatic charge mitigation devices, flame retardants, and electromagnetic interference (EMI) shielding.[8–13]

Shielding of electromagnetic (EM) radiation is of major concern due to more and more growing use of electronic equipment in our daily life. The use of metal sheets as a shielding material is disadvantageous because of heavy weight, processing problem, lack of flexibility, prone to oxidation, and leakage of radiation through the seams. It is evident that usually conductive materials can serve the purpose of EMI shielding. An intrinsically conducting polymer[14–16] can serve the purpose of EMI shielding material but it suffers from poor processability, environmental stability, high cost, and lack of mechanical properties.

Extrinsically electrically conducting polymer composites are lighter in weight, easy in processing, cost effective, and seams can either be reduced or completely eliminated by molding.[13] For efficient shielding, the conducting filler in polymer composites should have small size, high conductivity, and large aspect ratio.[17] Nanosized fillers have been reported to provide reasonable shielding effectiveness (SE) at very low content as compared to the traditional fillers.[18,19]

The mechanism of EMI shielding in a conducting composite differs from the shielding mechanism in a homogeneous material. In single phase material such as ferrite or metal, the attenuation of EM waves is either solely through absorption or solely through reflection. But in case of two phase system such as conducting polymer or cement composite, the attenuation of EM wave is through absorption, reflection, and multiple reflections.[17,20–23] Thus the total shielding effectiveness (SE) is the summation of SE due to the three independent phenomena. In past few decades, several works on EMI shielding of conducting

composites have been reported, but in most cases, the study has been restricted to the total SE.[13,24–26] Some researchers have evaluated the contribution of absorption and reflection towards the total SE.[27–29] But the correlation of these parameters with reflectance, absorbance, and transmittance has been scarcely analyzed.[30] In this article, we report the EMI shielding properties of MWCNT/PS composites in terms of SE due to reflection and absorption as well as reflectance, absorbance, and transmittance, with the aim of make an attempt to clarify the physical phenomena behind the shielding process in such composites.

Carbon nanotube (CNT) is promising nanosized filler which has shown to enhance the properties of the host polymer matrix due to its aforesaid special features in addition to high strength and low density.[31] The percolation threshold is marked by a drastic change in conductivity which is originated due to a formation of network of conductive pathways. This threshold is acknowledged as inversely proportional to the aspect ratio of CNT.[32] Recently, extremely low percolation threshold has been reported by several researchers.[33–35] It has been noticed that the percolation threshold is strongly dependent on dispersion of conducting filler in the polymer matrix[36,37] in addition to processing technique.[38] Appropriate dispersion of CNTs within the matrix is essential for achievement of lower percolation threshold.[39] Meaningful distribution of CNTs is not easy because of their agglomeration tendency.[40,41] Conductivity increases by increase in filler loading of unmodified CNT in natural rubber (NR) with an abrupt increase at percolation threshold; however functionalized CNT shows lower conductivity of composites compared with the unfuctionalized.[42] Studies reveal that the functionalization causes improvement in dispersion of CNT in NR matrix, which leads to reduction in electrical conductivity of CNT/NR composites. This is indorsed to preferential dispersion of filler in composites.

Many attempts have been made by researchers to determine methods that can enhance the dispersion of CNTs in polymer. Yet efficient processing method is still an important goal to achieve the complete potential of CNTs. Generally, two types of procedures have been referred to produce CNT/polymer nanocomposites.[9,10,43,44] First method involves the addition of CNTs into melted polymer matrix or polymer solution followed by mechanical mixing. Second is through chemical reaction between modified CNTs and polymer matrix. These methods have limitations such as difficulty in dispersion due to viscosity of polymer melts[45] and reagglomeration of the nanotubes during the drying process.[46,47] In this work, MWCNTs are dispersed in PS powder by means of tumble mixing in dry state, followed by pellet making through hot compression. Pellets so obtained are investigated for electrical, EMI shielding and mechanical properties.

EXPERIMENTAL

Materials

MWCNTs were obtained from Sigma Aldrich Ltd. Catalog Number: 677248-5G. Specification: > 99% carbon basis, inner diameter, outer diameter, length and density were ~2–6 nm, ~10–15 nm, 0.1–10 μm and 1.7–2.1 g/mL at 25°C, respectively. Polystyrene (PS) was used as matrix. The granules of PS were pulverized cryogenically. Particles size was found to be ~50–106 μm. For preparation of PS pellets, the powder was heated in a piston cylinder assembly at 115°C for some time, brought back to 90°C and then compressed at 75 MPa pressure for 15 min. The density of PS pellets was 1.0384 g cm^{-3} by considering the ratio of its weight to volume. It was evaluated precisely using micro scale measurements of sample's volume and weight. The observed conductivity of PS pellets was 6.9×10^{-16} S cm^{-1}.

Sample Preparation

MWCNT/PS nanocomposite samples were prepared using tumble mixing and subsequent compression molding at elevated temperature. Tumble mixer consisted of a variable speed rotating metallic stirrer in a tumbler along with heating provision. The mixture powder of MWCNTs and PS was rotated in the tumbler for 200 min. Initial low speed was followed by high speed. The idea is, first to break up the MWCNT agglomerates at low speed and subsequent dispersing of MWCNTs in PS matrix by means of high speed. The mixture powder of PS and MWCNTs was subjected to dispersal due to impacts with the stirrer and the walls of the tumbler. Embedding/filming of the MWCNTs onto the PS particles by high impact forces and the friction heat are obvious. Prolonged tumble mixing supposed to evenly disperse the MWCNTs in PS matrix, besides coating on PS particles, thus realizing strong interfacial bonding between the MWCNTs and the matrix. The resultant mixture was heated in a piston cylinder assembly at 115°C for some time, brought back to 90°C and then compressed at 75 MPa pressure for 15 min, similar to preparation of virgin PS pellets. A series of rectangular pellets with content 0.05–5 wt % of MWCNT in PS were prepared. Five pellets of each composition were made ready. The pellets prepared were of X-band waveguide size (22.86×10.16 mm^2) so as to fit in it precisely. The thicknesses of the pellets were between 2 and 3 mm.

Electrical measurements of specimen pellets were carried out in sand-witch geometry. SEM grade silver was painted on both surfaces for electrodes. For resistances below 200 MΩ, Keithley 2400 electrometer was used, while high resistances measurements were carried out by Keithley pico-ammeter. D Shore hardness tester was utilized for hardness measurements. The data reported here is the mean value. The return loss (RL) and SE were measured using WILTRON Vector network Analyzer. Zeiss Scanning Microscope was employed for SEM studies provide high resolution for the measurements under high vacuum.

Theory of EMI Shielding

EMI shielding theory is based on the terms reflectance (R), transmittance (T), and absorbance (A), which respectively refer to the fraction of incident power reflected, transmitted, and absorbed. Insertion loss describes the number of decibels the transmitted power is below the incident power, and in other words, it defines amount of attenuation archetypal of a particular material. Hence it is the same as (SE) which signifies the efficacy of a barrier to shield EM waves, and is written as $\mathrm{SE\ (dB)} = -10 \log_{10} T$. Return loss (RL) is a way to express the reflectance in terms of decibels and quantifies the number of decibels that the reflected signal is below the incident signal. It is written as $\mathrm{RL\ (dB)} = -10 \log_{10} R$. Absorbance can be described by the relation $A = 1 - R - T$.

As stated, three independent phenomena account to EM wave attenuation in case of conducting composites, which are

reflection, absorption and multiple reflections. Reflection is a surface phenomenon which occurs due to reflection of waves from the surface of the barrier when the waves encounter conducting particles. Absorption is a volume phenomenon which occurs due to conversion of EM energy into heat. Multiple reflections occur due to reflection of waves by the interfaces within the barrier. They can be ignored when the absorption loss is high.[20,27,51] The overall mechanism can be quantified in the following manner: when an EM wave encounters a barrier, a fraction of it gets reflected from the surface; the rest penetrates into the barrier, which would be absorbed and remaining transmitted. Effective absorbance (A_{eff}) refers to the fraction of penetrated power ($1 - R$) which is absorbed, and is the ratio of power absorbed to the power penetrated. Thus effective absorbance is the terminology which signifies how much the volume of the material is absorptive, disregarding the reflections at the surface. If P_{abs} is the absorbed power density, P_{inc} is the incident power density, P_{ref} is the reflected power density and P_{pen} is the power density of the wave which penetrates into the shield, then $P_{pen} = P_{ref} - P_{inc}$, and $A_{eff} = \frac{P_{abs}}{(P_{pen})} = \frac{A}{1-R}$.[30]

RESULTS AND DISCUSSION

Conductivity

The aim of this work is to develop electrically conductive PS nanocomposites with small amount of MWCNTs for achieving good EMI shielding properties while retaining mechanical strength. The dc conductivity (σ) behavior of these nanocomposites is illustrated as a function of the MWCNT loading in Figure 1. The variation of σ is similar in nature as cited in literature.[2,11,35,41,48] The curve is "*S*" shaped by inclusion of samples in the low range between 0 and 0.1 wt % MWCNT for example with 0.02 wt % loading, unlike to composites with other fillers[49,50] (in Figure 1, "*S*" shape is not duly picture-perfect due proximity of conductivity values). The σ of PS increases abruptly by about twelve orders of magnitude from 6.8×10^{-16} S/cm to 9.9×10^{-4} S/cm on addition of 0.1 wt % MWCNTs. The major rise of eight orders occurs on addition of 0.05 wt % MWCNTs under the anti-static range and drops to 9.9×10^{-4} S/cm under semiconductor range. This can be attributed to the formation of a network of conductive paths. These conductive channels consist of MWCNTs. The electrical conduction is supposed to take place by inter-MWCNT contacts, as well as electrons hopping/tunneling across the gaps or energy barriers between conducting MWCNTs in PS matrix. When the distance between conductive components within the PS matrix is close to an edge value usually a few nanometers, quantum mechanical tunneling is expected to take place. The σ appears to be unvarying over higher concentration of MWCNT. With the addition of MWCNTs from 0.2 to 5 wt %, the curve flattens with a marginal rise in σ from 2.63×10^{-3} S cm^{-1} to 7.98×10^{-3} S cm^{-1}. This suggests that additional increase in MWCNTs does not significantly improve the overall σ of nanocomposite.

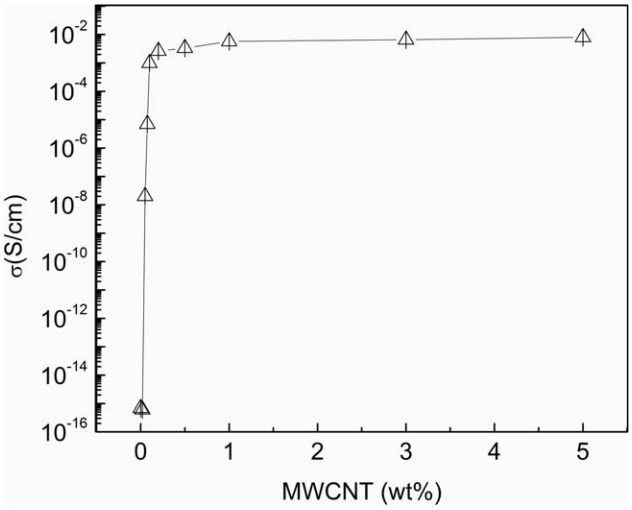

Figure 1. Variation of conductivity as a function of MWCNT loading in PS matrix.

The increase in σ of PS with MWCNTs loading can be explained in terms of general mechanism of conduction for extrinsically conductive systems.[52] Extended tumble mixing expected to reliably disperse the MWCNTs in PS matrix due to high impacts forces with the stirrer and walls of the tumbler in addition to coating on PS particles. It is during pellet formation at elevated temperature, conductive filler (MWCNTs) in molten PS matrix leads to formation of discrete conductive aggregates which grows into continuous conductive paths at critical concentration known as percolation threshold. Progressive increase in MWCNTs above percolation would only increase the number of such paths leading to formation of conductive network mesh. Consequently the increase in conductivity becomes marginal. Initial abrupt increase in σ from insulating to antistatic range can be ascribed to beginning of formation of a network of conductive paths of MWCMTs due to hopping and quantum mechanical tunneling of electrons therein. Therefore, it is logical to consider this as the percolation threshold. It is noteworthy to mention that the percolation threshold/critical concentration of conductive filler formed is very much dependent on certain characteristics of conductive filler, dispersion in polymer matrix,[36,37] and processing technique.[38] Homogenous distribution of MWCNTs is not easy because of their agglomeration tendency.[40,41]

The σ of a composite is typically ascribed to morphology of the filler and its dispersion in the matrix.[13] Depending on dispersion in matrix, 15–25 wt % of carbon black (particle nature) and 10–15 wt % of carbon fiber (rod shape) normally display the percolation threshold.[20,49] The MWCNTs have shown percolation threshold with small mass content of 0.08 wt % due to their typically high aspect ratio.[35] While in this work, a quite low value of 0.05 wt % MWCNTs in PS matrix has shown the percolation threshold. Such a low mass fraction of MWCNTs for percolation threshold may be endorsed to the processing technique used in this work, which has already been recognized for graphite/polymer composites.[38] Conducting network configuration through MWCNTs string can be a key aspect in lowering the percolation limit. This is being revealed in scanning electron microscope (SEM) studies.

Scanning Electron Microscopy

Magnification 10,000×. All specimen pellets were freeze fractured into two pieces using liquid nitrogen. Micrographs (a)–(d) in Figure 2 show the cross sectional view of one part of

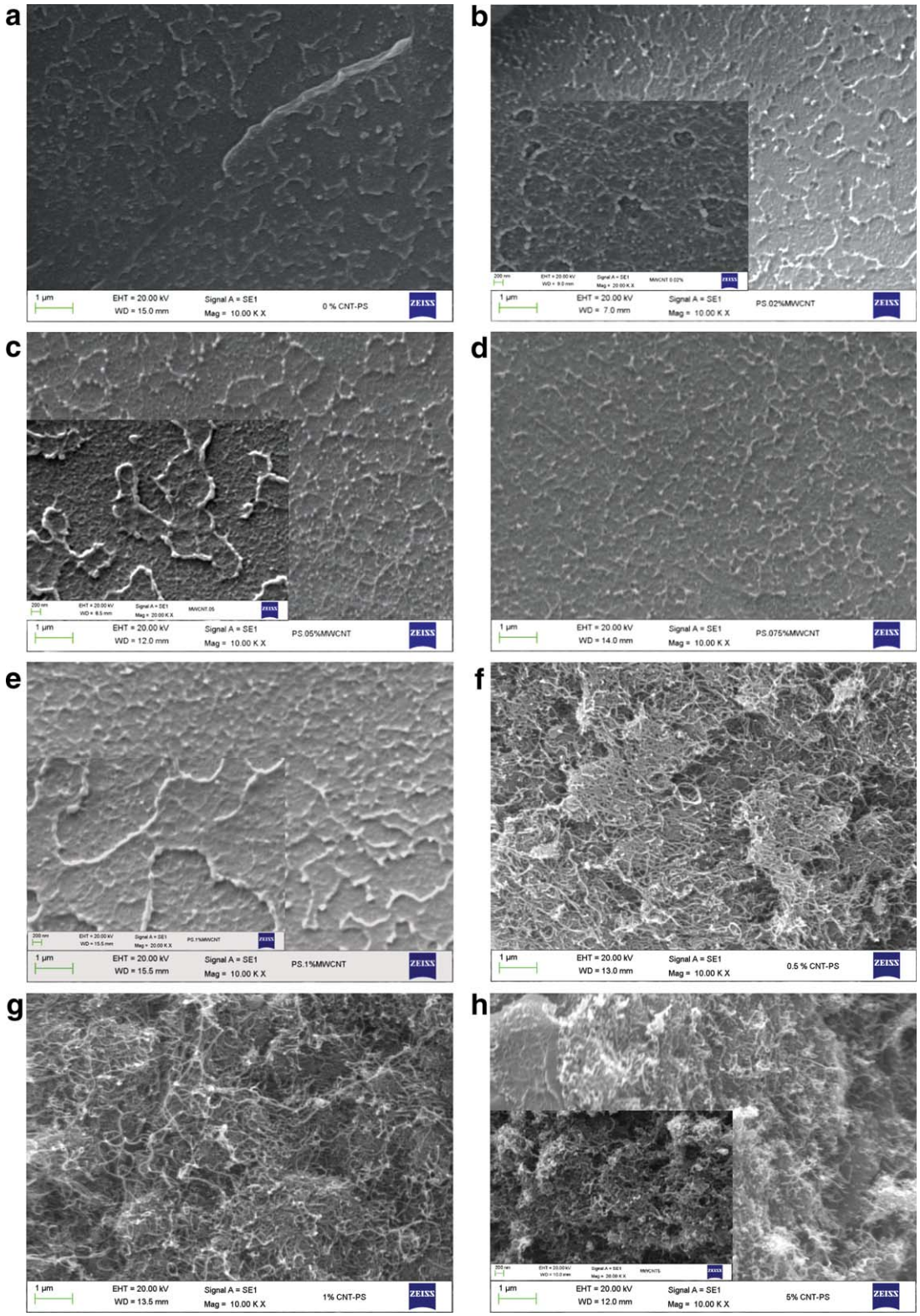

Figure 2. SEM micrographs magnification ×10,000 (a) pristine PS; PS composites with MWCNT (b) 0.02 wt %, inset at magnification ×20,000; (c) 0.05 wt %, inset at magnification ×20,000; (d) 0.075 wt %; (e) 0.1 wt %, inset at magnification ×20,000; (f) 0.5 wt %; (g) 1.0 wt %; (h) 5.0 wt %, inset at magnification ×20,000. [Color figure can be viewed in the online issue, which is available at wileyonlinelibrary.com.]

freeze fractured pellets of pristine PS and PS composites having 0.02, 0.05, 0.075, 0.1, 0.5, 1.0, and 5.0 wt % of MWCNTs at 10,000 × magnification. Figure 2(a) displays the texture of pristine PS with spots of scraps of other part of fractured pellet. Figure 2(b–h) depicts the formation of pathways/channels of MWCNTs in composites with 0.02–5.0 wt % MWCNTs. One

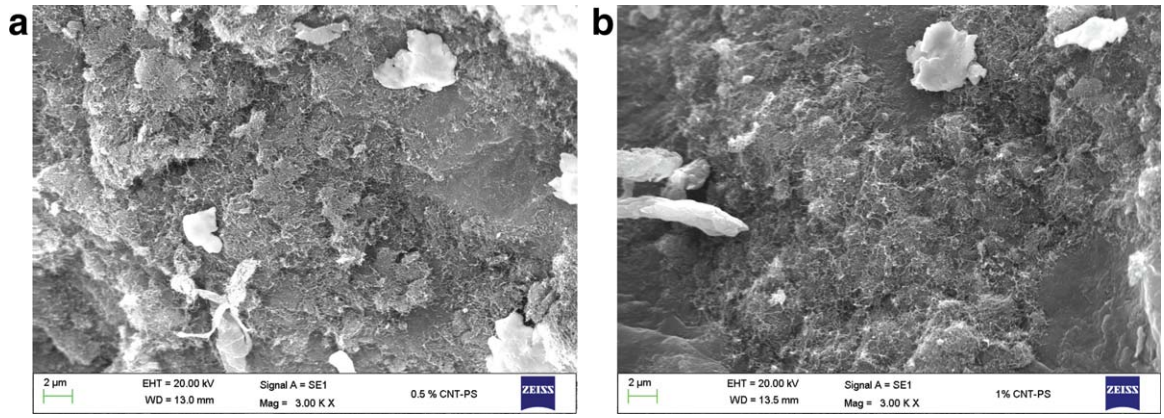

Figure 3. SEM micrographs magnification ×3000, PS composites with MWCNT (a) 0.5 wt %; (b) 1.0 wt %. [Color figure can be viewed in the online issue, which is available at wileyonlinelibrary.com.]

can observe these even in low MWNTs composites by zooming. Inset Figure (b,c,g) at magnification 20,000× confirm the statement. In samples with extremely low content of MWCNTs in PS keeps pathways embedded inside the composites since the spread volume of MWCNTs in PS is less than PS, while in composite with higher content of MWCNTs the channels are distinct due to large volume of dispersed MWCNTs in PS, besides coating of PS on MWCNTs. In fact in a composite with high MWCNTs loading of 0.5–5.0 wt % there is formation of mesh of conductive networks. Stacking of multiple channels is apparent in composites with increasing content of MWCNTs predominantly in composite with 5.0 wt % MWCNTs. This situation can be visualized as follows: with the increase in filler content the number of conductive mesh increases and they are randomly placed in the system one after another in higher content samples. Therefore, with continuous increase in filler the number of mesh increases and resulting more and more increase in SE.

Web/mesh-like structure consisting of MWCNTs within PS matrix can be clearly noticed particularly in composites of high MWCNTs content micrographs. Obviously these webs are part of network of conducting pathways/channels. This implies that formation of web/mesh structure consisting of MWCNTs has played an important role in the improvement of electrical property of these composites. Very low percolation threshold in these composites thought to be the result of such structure.

Magnification 3000×. To make sure of web/mesh structure in whole of composite, a wide view of freeze fractured pellets of PS composites having 0.5 and 1.0 wt % MWCNTs have been illustrated in micrographs (a) and (b) in Figure 3 at lower magnification 3000×. Webs are distinctly visible by zooming. These webs consist of conductive MWCNTs. Such type of structure has the capability to block external electric fields like Faraday shield consisting of mesh of conducting material.

EM Shielding

SE and RL were determined through S11/S22 and S12/S21 scattering parameters of two port vector network analyzer. *R*, *T*, *A*, and A_{eff} were determined using the above relations. Table I summarizes the attenuation of EM radiations as a result of *R* and *A* for various compositions of MWCNT/PS composites in X-band frequency range. Total attenuation of EM radiations increases with the rise of MWCNT level in PS composites. *R* is in increasing order with the enhancement of MWCNT content since the EM waves encounter with more conducting particles and get reflected. Evaluated values A_{eff} at 9 GHz in Table II reveal its increase with rising of MWCNT content together with dominance compared with *R*. A_{eff} is 97% compared with 78%

Table I. Evaluated Values of "*R*," "*A*," and "*T*"

MWCNT wt %	0.1			0.2			0.5			5		
Freq. (GHz) ↓	*R* %	*A* %	*T* %	*R* %	*A* %	*T* %	*R* %	*A* %	*T* %	*R* %	*A* %	*T* %
8.5	24.9	19.8	55.3	32.5	27.2	40.3	50.2	28.7	21.1	83.5	15.9	0.6
9	22.9	18.1	59.0	29.9	26.4	43.7	47.0	30.7	22.3	78.1	21.3	0.6
9.5	26.1	20.5	53.4	31.9	26.6	41.5	46.2	32.7	21.1	73.1	26.4	0.5
10	23.3	20.3	56.4	31.2	26.3	42.5	43.0	35.1	21.9	68.0	31.5	0.5
10.5	22.5	18.7	58.8	30.0	25.7	44.3	41.1	36.5	22.4	64.6	34.9	0.5
11	24.7	18.4	56.9	29.7	26.0	44.3	37.8	39.3	22.9	59.4	40.1	0.5
11.5	22.9	23.9	53.2	27.3	29.3	43.4	33.6	43.1	23.3	55.6	43.9	0.5
12	16.6	8.9	74.5	24.0	16.7	59.3	31.3	39.0	29.7	50.8	48.7	0.5
Thickness (mm)		2.92			2.92			2.40			2.60	

Table II. Evaluated Values of "*R*," "*A*," "A_{eff}," and "*T*" at 9 GHz

MWCNT wt %	*R* %	*A* %	A_{eff}%	*T* %
0.1	22.9	18.1	23.4	59
0.2	29.9	26.4	37.6	43.7
0.5	47.0	30.7	57.9	22.3
1	39.1	31.9	52.3	29.0
3	70.8	26.5	90.6	2.8
5	78.1	21.3	97.4	0.6

of *R* in case of 5 wt % MWCNT nanocomposite, which suggests that the material is absorptive.

Shielding Effectiveness. The total SE can be written as $SE = SE_{ref} + SE_{abs} + SE_{mult}$. Here SE_{ref} is the attenuation due to reflection, SE_{abs} is the attenuation due to absorption, and SE_{mult} is the attenuation due to multiple reflections. As stated above, multiple reflections can be ignored due to high absorbance. Therefore, $SE = SE_{ref} + SE_{abs}$. Neat PS is transparent for EM radiations. Understandably its total SE would be zero. Figure 4 shows the total SE of MWCNT/PS composites for various compositions as a function of frequency. The uncertainty in measurements was ±0.04 dB.

SE is found to be almost independent of frequency in the X band. The figure illustrates the rise in SE with enhancement of MWCNT content. Composite containing very small amount of 0.5 wt % MWCNTs shows an SE of ~7 dB and 23.5 dB is observed with 5 wt % MWCNTs. The conductivity data and the micrographs have revealed that increasing content of MWCNTs decreases the distance between conductive components in PS matrix. Consequently, more EM waves encounter with additional MWCNTs, and hence MWCNT rich areas attenuate more radiation as compared with PS rich areas, making an increase in SE with increasing MWCNT concentration. The SE increases

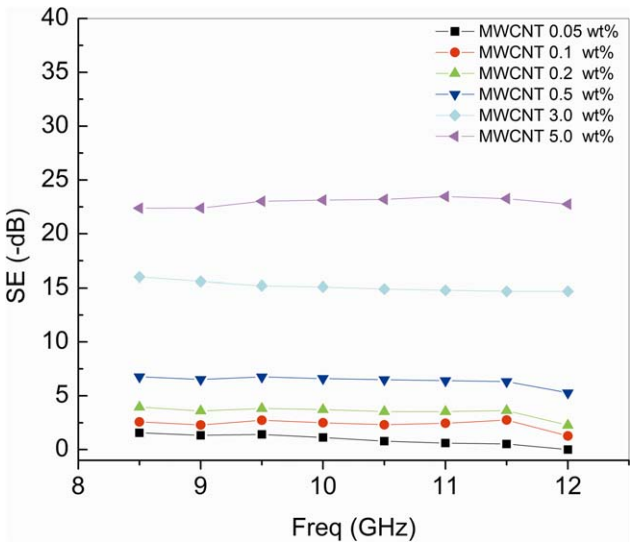

Figure 4. Variation of SE as a function of frequency for various compositions of MWCNT/PS composites. [Color figure can be viewed in the online issue, which is available at wileyonlinelibrary.com.]

first slowly and then rapidly with increasing MWCNT content. This is in contrast to the conductivity behavior which increases rapidly at lower MWCNT content followed by saturation on addition of 0.2 wt % MWCNT. This indicates that only conductivity is not the decisive factor for managing the degree of SE, some additional factor also plays a significant role. The reason can be endorsed to the conducting mechanism which requires connectivity between conductive pathways, whereas shielding does not.[17] As such insulating polymer matrix is transparent to incident radiation. SE of metals is due to reflection while of conductive composite is normally due to absorption. Additionally, SE also depends on the formation of close packed conductive networks in the polymer composites[14] which increases with the increase in filler loading in the polymer composite. The conductive network formed due to addition of conductive filler interacts with incident ray and also a source for SE. In SEM micrographs (Figure 2) in composites with high MWCNTs content (above percolation), there is formation of mesh of conductive network. As visualized,[14] the increase in filler loading closely packs the conductive mesh network. Therefore, their ability to absorb electromagnetic radiation increases and consequently the SE increases. It is noteworthy that the addition of MWCNTs from 0.2 to 5 wt % in PS composites provides a negligible rise in σ from 2.63×10^{-3} S cm^{-1} to 7.98×10^{-3} S cm^{-1}, which suggests that additional increase in MWCNTs make available a close packed conductive network. Additionally, conductive mesh of MWCNTs as observed in micrographs give rise to an extra attenuation of EM radiation like Faraday shield consisting of mesh of conducting material which has the capability to block external electric fields. As observed in the micrographs, these meshes are also a part of network of conductive channels, and since the Stacking of multiple channels increases with the addition of MWCNTs, there is a net rise in SE with rising filler content. Hence, MWCNT/PS composites processed through technique used in this work demonstrate comparatively improved values of SE than using solution mixing method.[18,19,53] Comparison of SE data in Table III confirms the finding.

Return Loss. Variation of return loss (RL) as a function of frequency is illustrated in Figure 5. As expected, the composites having a high value of SE exhibited lower value of RL. The RL was found to be increasing with frequency except for lower MWCNT loadings of 0.05 wt % and 0.1 wt %. The random variation of RL with frequency in these two composites with lower

Table III. Comparison of SE with Other's Work

Composite	MWCNT (wt %)	SE (−dB)	Processing method
MWCNT/ PS Foam (Ref. 45)	7	19.3	Solution mixing
MWCNT/ PS (Ref. 13)	1	7.9	Solution mixing
MWCNT/ PS (Ref. 12)	7	26	Solution mixing
MWCNT/PS (This work)	5	23.5	Dry tumble mixing
	3	16	
	0.5	~7	

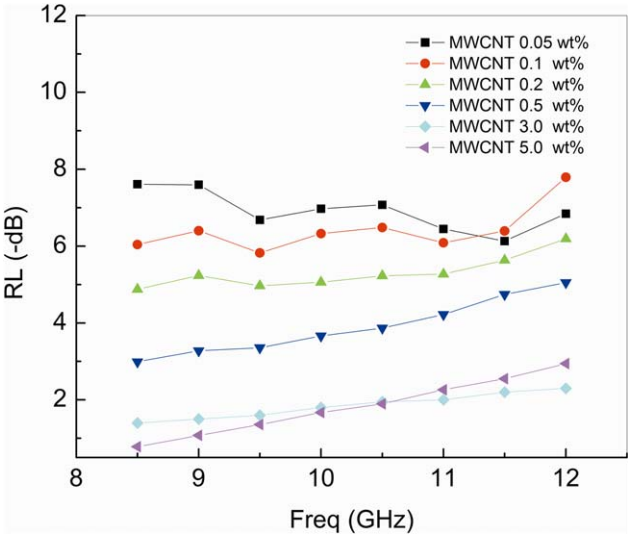

Figure 5. Variation of RL as a function of frequency for various compositions of MWCNT/PS composites. [Color figure can be viewed in the online issue, which is available at wileyonlinelibrary.com.]

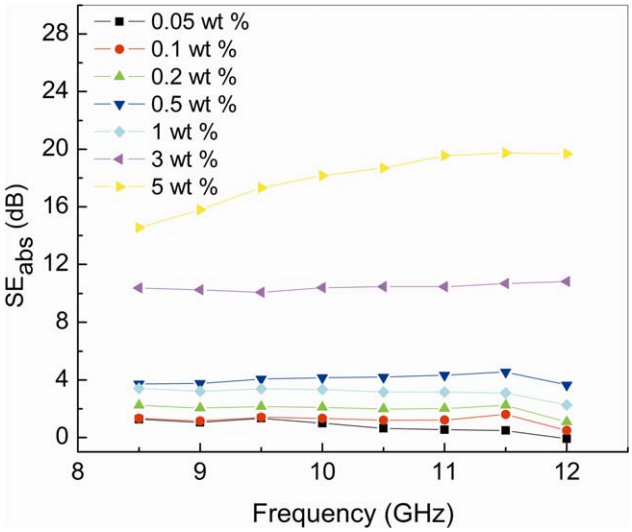

Figure 7. Variation of SE_{abs} as a function of frequency for various compositions of MWCNT/PS composites. [Color figure can be viewed in the online issue, which is available at wileyonlinelibrary.com.]

concentration MWCNTs can be attributed to interaction of wave with probability of voids formation during processing of these composites.[20]

Shielding Effectiveness Due to Reflection and Absorption. Figures 6 and 7 show the contribution of reflection (SE_{ref}) and absorption (SE_{abs}) to the total SE where $SE = SE_{ref} + SE_{abs}$. SE_{ref} can be determined by expressing the power that could not be reflected in terms of dB, to be precise, by expressing $(1 - R)$ in terms of dB. $SE_{ref} = -10\log_{10}(1-R)$. SE_{abs} can be determined by expressing the penetrated power that could not be absorbed in terms of dB. $SE_{abs} = -10\log_{10}(1-A_{eff}) = -10\log_{10}\left\{\frac{T}{(1-R)}\right\}$.[30] The evaluated SE_{abs} is in good agreement with the value obtained through the relation $SE_{abs} = SE - SE_{ref}$.

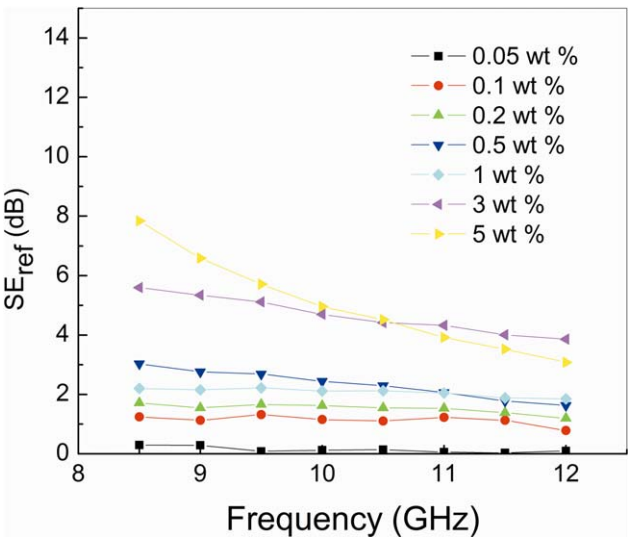

Figure 6. Variation of SE_{ref} as a function of frequency for various compositions of MWCNT/PS composites. [Color figure can be viewed in the online issue, which is available at wileyonlinelibrary.com.]

Both SE_{ref} and SE_{abs} almost remain constant with frequency, except for the sample with 5 wt % MWCNT, in which the SE_{ref} slightly decreases with increase in frequency and SE_{abs} increases. This variation is within the limits of the error in measurement. The same trend had been observed for *R*, *A*, and *T* in Table II. It is evident that the contribution of absorption to the total SE is larger than reflection, which was also demonstrated in Table II. Thus, though reflectance is higher than absorbance, absorption mechanism is intrinsically dominated in MWCNT/PS composites.

Hardness

Figure 8 shows the variation of shore D hardness with composition. The hardness of PS virgin pellet is 80 on 100 scale of shore D hardness, which decreases to 75 in case of composite with 1 wt % MWCNTs followed by 69 for composite with 5 wt %

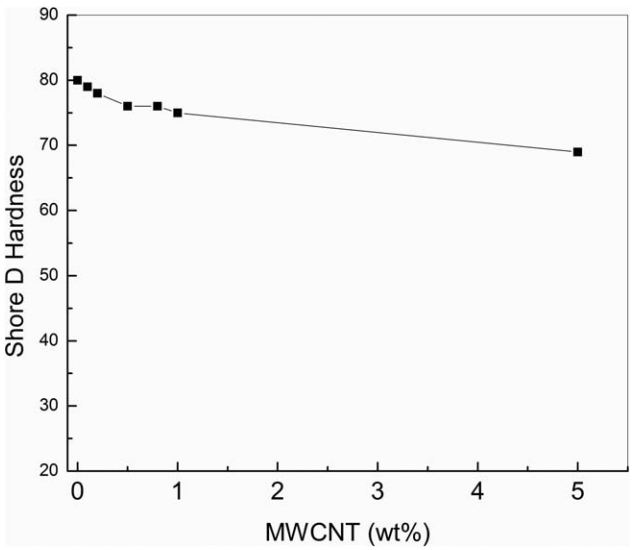

Figure 8. Variation of shore D hardness as a function of filler content.

MWCNTs. A marginal decrease in hardness implies that addition of MWCNTs in the PS has not prevented the inter-particles merger of matrix. It also indicates strong interfacial bonding between MWCNTs and PS matrix. Nanocomposites with such pragmatic hardness can with stand any product application.

CONCLUSIONS

Dispersion of MWCNTs in PS powder via tumble mixing method with subsequent compression molding of nanocomposites at elevated temperature has proved to be helpful for achievement of better results. Extremely low content of 0.05 wt % MWCNTs in PS composite for percolation threshold has rarely been realized by other researchers. Comparative analysis of SE with reported values using solution mixing technique in the literature has confirmed the realization of higher SE with low MWCNT content. Study of R, A, T, A_{eff}, SE_{ref}, and SE_{abs} suggests that the shielding is absorption dominated. Improved properties with lower MWCNTs loading are undoubtedly better compared with carbon fiber and carbon black-filled polymer composites. The required EMI shielding of the conductive composites for different electronic devices is about 15–20 dB. Thus, PS composite with 5 wt % MWCNTs having ~23.5 dB SE appears to be promising for its commercial use as shielding material. Small decrease in shore D hardness with increase in MWCNT content implies its realistic application. Composite containing 0.5 wt % of MWCNTs which has demonstrated SE ~ 7 dB can be utilized in application where static charge dissipation is significant.

This research is financially supported under Govt. of India UGC project F. No. 32–41/2006 (SR). Thank to Prof. D. Pental (Vice Chancellor) for permission to execute this project in the Department of Physics and Astrophysics, University of Delhi.

REFERENCES

1. Spitalsky, Z.; Tasis, D.; Papagelis, K.; Galiotis, C. *Prog. Polym. Sci.* **2010**, *35*, 357.
2. Al-Saleh, M. H.; Sundararaj, U. *Carbon* **2009**, *47*, 2.
3. Verdejo, R.; Bernal, M. M.; Romasanta, L. J.; Lopez-Manchado, M. A. *J. Mater. Chem.* **2011**, *21*, 3301.
4. Potts, J. R.; Dreyer, D. R.; Bielawski, C. W.; Ruoff, R. S. *Polymer* **2011**, *52*, 5.
5. Rahaman, M.; Thomas, S. P.; Hussein, I. A.; De, S. K. *Polym. Compos.* **2013**, *34*, 494.
6. Sohi, N. J. S.; Rahaman, M.; Khastgir, D. *Polym. Compos.* **2011**, *32*, 1148.
7. Magioli, M.; Soares, B. G.; Sirqueira, A. S.; Rahaman, M.; Khastgir, D. *J. Appl. Polym. Sci.* **2012**, *125*, 1476.
8. Ruan, S. L.; Gao, P.; Yang, X. G.; Yu, T. X. *Polymer* **2003**, *44*, 5643.
9. Coleman, J. N.; Cadek, M.; Blake, R.; Nicolosi, V.; Ryan, K. P.; Belton, C.; Fonseca, A.; Nagy, J. B.; Gun'ko, Y. K.; Blau, W. *J. Adv. Funct. Mater.* **2004**, *14*, 791.
10. Jell, G.; Verdejo, R.; Safinia, L.; Shaffer, M. S. P.; Stevens, M. M.; Bismarck, A. *J. Mater. Chem.* **2008**, *18*, 1865.
11. Smith, J. G.; Connell, J. W.; Delozier, D. M.; Lillehei, P. T.; Watson, K. A.; Lin, Y.; Zhou, B.; Sun, Y. P. *Polymer* **2004**, *45*, 825.
12. Peeterbroeck, S.; Laoutid, F.; Taulemesse, J. M.; Monteverde, T.; Lopez-Cuesta, J. M.; Nagy, J. B.; Alexandre, M.; Dubois, P. *Adv. Funct. Mater.* **2007**, *17*, 2787.
13. Das, N. C.; Maiti, S. *J. Mater. Sci.* **2008**, *43*, 1920.
14. Rahaman, M.; Chaki, T. K.; Khastgir, D. *J. Mater. Sci.* **2011**, *46*, 3989.
15. Wang, Y.; Jing, X. *Polym. Adv. Tech.* **2005**, *16*, 344.
16. Jing, X.; Wang, Y.; Zhang, B. *J. Appl. Polym. Sci.* **2005**, *98*, 2149.
17. Chung, D. D. L. *Carbon* **2001**, *39*, 279.
18. Yang, Y. L.; Gupta, M. C.; Dudley, K. L.; Lawrence, R. W. *J. Nanosci. Nanotechnol.* **2005**, *5*, 927.
19. Yang, Y.; Gupta, M. C.; Dudley, K. L. *Nanotechnology* **2007**, *18*, 345701.
20. Das, N. C.; Khastgir, D.; Chaki, T. K.; Chakraborty, A. *Compos. Part A-Appl. S* **2000**, *31*, 1069.
21. Luo, X. C.; Chung, D. D. L. *Compos. Part B-Eng* **1999**, *30*, 227.
22. Wright, J. R.; Burns, M. K.; James, E.; Sloan, M. R.; Evans, K. E. *Text. Res. J.* **2012**, *82*, 645.
23. Kim, H. M.; Kim, K.; Lee, C. Y.; Joo, J.; Cho, S. J.; Yoon, H. S.; Pejakovic, D. A.; Yoo, J. W.; Epstein, A. *J. Appl. Phys. Lett.* **2004**, *84*, 589.
24. Das, N. C.; Yamazaki, S.; Hikosaka, M.; Chaki, T. K.; Khastgir, D.; Chakraborty, A. *Polym. Int.* **2005**, *54*, 256.
25. Das, N. C.; Liu, Y. Y.; Yang, K. K.; Peng, W. Q.; Maiti, S.; Wang, H. *Polym. Eng. Sci.* **2009**, *49*, 1627.
26. Huang, Y.; Li, N.; Ma, Y. F.; Feng, D.; Li, F. F.; He, X. B.; Lin, X.; Gao, H. J.; Chen, Y. S. *Carbon* **2007**, *45*, 1614.
27. Grima, J. N.; Chetcuti, E.; Manicaro, E.; Attard, D.; Camilleri, M.; Gatt, R.; Evans, K. E. *P R Soc. A* **2012**, *468*, 810.
28. Sachdev, V. K.; Patel, K.; Bhattacharya, S.; Tandon, R. P. *J. Appl. Polym. Sci.* **2011**, *120*, 1100.
29. Sachdev, V. K.; Srivastava, N. K.; Kumar, K.; Mehra, R. M. *Mater. Sci.-Poland* **2005**, *23*, 269.
30. Hong, Y. K.; Lee, C. Y.; Jeong, C. K.; Lee, D. E.; Kim, K.; Joo, J. *Rev. Sci. Instrum.* **2003**, *74*, 1098.
31. Breuer, O.; Sundararaj, U. *Polym. Compos.* **2004**, *25*, 630.
32. Potschke, P.; Bhattacharyya, A. R.; Janke, A. *Polymer* **2003**, *44*, 8061.
33. Sandler, J. K. W.; Kirk, J. E.; Kinloch, I. A.; Shaffer, M. S. P.; Windle, A. H. *Polymer* **2003**, *44*, 5893.
34. Lisunova, M. O.; Mamunya, Y. P.; Lebovka, N. I.; Melezhyk, A. V. *Eur. Polym. J.* **2007**, *43*, 949.
35. Shrivastava, N. K.; Khatua, B. B. *Carbon* **2011**, *49*, 4571.
36. Kodgire, P. V.; Bhattacharyya, A. R.; Bose, S.; Gupta, N.; Kulkarni, A. R.; Misra, A. *Chem. Phys. Lett.* **2006**, *432*, 480.
37. Hu, G. J.; Zhao, C. G.; Zhang, S. M.; Yang, M. S.; Wang, Z. G. *Polymer* **2006**, *47*, 480.
38. Bhattacharya, S.; Tandon, R. P.; Sachdev, V. K. *J. Mater. Sci.* **2009**, *44*, 2430.

39. Ji, L. J.; Stevens, M. M.; Zhu, Y. F.; Gong, Q. M.; Wu, J. J.; Liang, J. *Carbon* **2009**, *47*, 2733.
40. Slobodian, P.; Pavlinek, V.; Lengalova, A.; Saha, P. *Curr. Appl. Phys.* **2009**, *9*, 184.
41. Narh, K. A.; Agwedicham, A. T.; Jallo, L. *Powder Technol.* **2008**, *186*, 206.
42. Thomas, P. S.; Abdullateef, A. A.; Al-Harthi, M. A.; Atieh, M. A.; De, S. K.; Rahaman, M.; Chaki T. K.; Khastgir D.; Sri Bandyopadhyay, S. *J. Mater. Sci.* **2012**, *47*, 3344.
43. Andrews, R.; Jacques, D.; Minot, M.; Rantell, T. *Macromol. Mater. Eng.* **2002**, *287*, 395.
44. Wang, S.; Liang, R.; Wang, B.; Zhang, C. *Carbon* **2007**, *45*, 3047.
45. Narh, K. A.; Jallo, L.; Rhee, K. Y. *Polym. Compos.* **2008**, *29*, 809.
46. Chatterjee, T.; Yurekli, K.; Hadjiev, V. G.; Krishnamoorti, R. *Adv. Funct. Mater.* **2005**, *15*, 1832.
47. Gopakumar, T. G.; Xanthos, M.; Xanthos, M. *Polym. Compos.* **2006**, *27*, 368.
48. Li, N.; Huang, Y.; Du, F.; He, X. B.; Lin, X.; Gao, H. J.; Ma, Y. F.; Li, F. F.; Chen, Y. S.; Eklund, P. C. *Nano. Lett.* **2006**, *6*, 1141.
49. Foulger, S. H. *J. Appl. Polym. Sci.* **1999**, *72*, 1573.
50. Maaroufi, A.; Haboubi, K.; El Amarti, A.; Carmona, F. *J. Mater. Sci.* **2004**, *39*, 265.
51. Ramirez, M.; Sabina, F. *J. Eur. J Mech. a-Solid* **2012**, *32*, 59.
52. Pierre, D. R.; Perenboom, J. A.; Van Bentum, P. J. M. *Phys. Rev. B* **1990**, *42*, 3380.
53. Yang, Y. L.; Gupta, M. C. *Nano. Lett.* **2005**, *5*, 2131.